

Performance of Ultra-Fast Silicon Detectors

N. Cartiglia^{a*}, M. Baselga^{bc}, G. Dellacasa^a, S.Ely^{bd}, V. Fadeyev^b, Z. Galloway^b, S. Garbolino^a, F. Marchetto^a, S. Martoiu^a, G. Mazza^a, J. Ngo^b, M. Obertino^{ae}, C. Parker^b, A. Rivetti^a, D. Shumacher^b, H.F-W.Sadrozinski^b, A. Seiden^b, A. Zatserklyaniy^b

^a*INFN Torino,*

Via Pietro Giuria 1, Torino, Italia

E-mail: cartiglia@to.infn.it

^b*Santa Cruz Institute for Particle Physics*

UC Santa Cruz, CA, 95064, USA.

^c*Permanent address: Centro Nacional de Microelectronica, CNM-IMB (CSIC), Barcellona, Spain.*

^d*Permanent address: Dept. of Physics, Syracuse, Univ., Syracuse, NY 13210, USA.*

^e*Università del Piemonte Orientale, Novara, Italia.*

ABSTRACT: The development of Low-Gain Avalanche Detectors has opened up the possibility of manufacturing silicon detectors with signal larger than that of traditional sensors. In this paper we explore the timing performance of Low-Gain Avalanche Detectors, and in particular we demonstrate the possibility of obtaining ultra-fast silicon detector with time resolution of less than 20 picosecond.

KEYWORDS: detector; fast; silicon, timing.

*Corresponding author.

Contents

1. Introduction	1
1.1 Ultra-Fast Silicon Detectors	2
2. Time-Tagging detectors	2
2.1 Time Walk	3
2.1.1 Time Walk Mitigation Techniques	4
2.2 Jitter	4
3. A Parametrization of σ_t	5
3.1 Choice of Preamplifier Rise Time	6
4. Results	6
4.1 State of the Art	7
4.2 Ultra-Fast Silicon Detector	7
4.2.1 Additional Sources of Timing Errors	9
5. Summary	9

1. Introduction

The possibility to use and control charge multiplication in un-irradiated silicon detectors has been the subject of intense study within the RD50 collaboration [1]. The basic mechanism to obtain charge multiplication is to create, within the bulk of a silicon sensor, a large volume where the electric field is high enough so that the drifting electrons will generate a controlled, low gain avalanche. Charge multiplication in silicon detector follows, for a constant field, a typical exponential behaviour:

$$N(x) = N_o * e^{\alpha * x} = G * N_o, \quad (1.1)$$

where at a field $V = 270 \text{ kV/cm}$ the value of α for electrons is $\alpha_e \sim 0.7 \text{ pair}/\mu\text{m}$ while for holes is $\alpha_h \sim 0.1 \text{ pair}/\mu\text{m}$.

Low-gain avalanche detectors (LGAD), as develop by CNM [2, 3], are $n - on - p$ silicon sensors with a high ohmic p bulk which have a p^+ implant extending several microns underneath the n -implant. Figure 1 shows the $n^{++} - p^+ - p - n^{++}$ structure of a LGAD.

This implant generates a large local field at a depth of about $1 - 5 \mu\text{m}$. The doping concentration of the p^+ implant is chosen to generate a gain of 10-100, in contrast to a gain of 10^4 or more in silicon photomultipliers (SiPM) and multi-pixel photon counters (MPPC). LGAD sensors

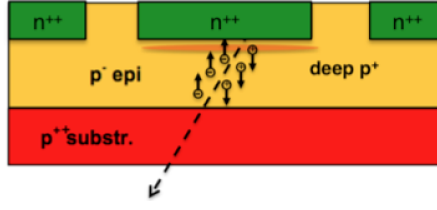


Figure 1. Schematic of a Low Gain Avalanche Diode. The extra deep p^+ layer creates a strong electric field that generates charge multiplication.

work by inducing multiplication for electrons, while the hole multiplication, given the field and depth values involved, is insignificant. Therefore, LGAD sensors do not have a positive feedback loop formed by the concurrent electron and hole multiplication processes, present in SiPM, which causes dead time after the avalanche.

1.1 Ultra-Fast Silicon Detectors

The design of ultra-fast silicon detectors (UFSD) [4, 5, 6] exploits the effect of charge multiplication in LGAD to obtain a silicon detector that can concurrently measure with high accuracy time and space. The development of UFSD will open up a range of new opportunities for applications that benefit from the combination of position and timing information. UFSD are the first detectors able to perform 4-dimensional tracking of charged particles with a very good space and time resolution: $\sigma_t \sim 10 - 30 \text{ ps}$, $\sigma_x \sim 20 - 50 \mu\text{m}$.

In its foreseen design, UFSD employs a dedicated ASIC chip for the read-out, in an hybrid configuration. The pixel size of UFSD needs to be large enough to house the necessary electronic circuits: currently we foreseen a minimum pixel size of $50\text{-}100 \mu\text{m}$, depending on the technology used for the ASIC design.

In the following we review the basic ingredients of a time-tagging detector and the state of the art of silicon detector timing. We propose a general parametrization of the timing characteristics of a detector and we use it to predict the timing performances of UFSD.

2. Time-Tagging detectors

Figure 2 shows the main components of a time-tagging detector. For a review of current trends in electronics see for example [7]. The silicon sensor, a pixel in the picture, is read-out by a pre-amplifier that shapes the signal. The shaper's output is then compared to a fixed threshold to determine the time of arrival. In the following we will use this simplified model to explore the UFSD timing capabilities, while we will not consider more complex and space-consuming approaches such as waveform sampling.

The time resolution σ_t can be expressed as the sum of three terms: (i) Time Walk , (ii) Jitter, and (iii) TDC binning:

$$\sigma_t^2 = \sigma_{TW}^2 + \sigma_J^2 + \sigma_{TDC}^2. \quad (2.1)$$

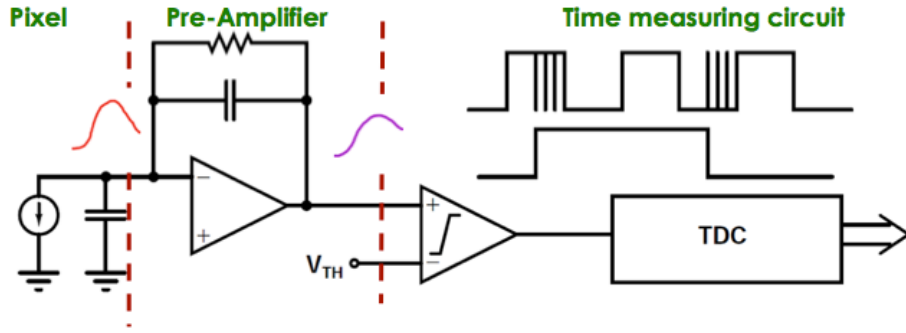


Figure 2. Main components of a time-tagging detectors. The time is measured when the signal crosses the threshold.

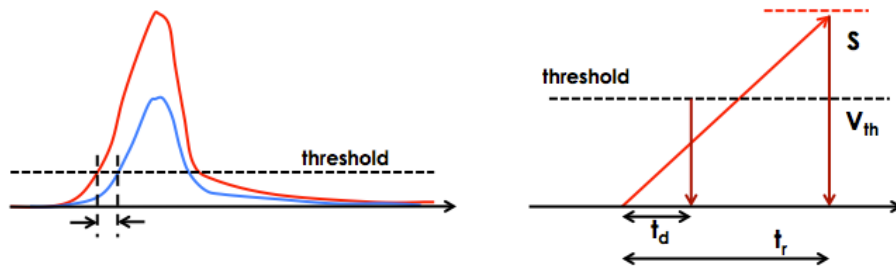


Figure 3. Left pane: Signals of different amplitude cross a fix threshold at different times, generating a delay on the on the firing of the discriminator that depends upon the signal amplitude. Right pane: a linear signal, with amplitude S and rise time t_r crosses the threshold V_{th} with a delay t_d .

TDC binning introduces a fix uncertainty equal to $\sigma_{TDC} = TDC_{bin}/\sqrt{12}$. As the performance of TDCs become faster and faster [7], we assume $TDC_{bin} = 20$ ps and therefore this effect will not be important.

2.1 Time Walk

The term *Time Walk* indicates the unavoidable effect that larger signals cross a given threshold earlier than smaller ones, Figure 3, left pane.

Let's assume for simplicity a linear signal, with amplitude S and rise time t_r . This signal crosses the threshold V_{th} with a delay t_d , Figure 3, right pane. From the following identity $t_d : t_r = V_{th} : S$ we can derive:

$$t_d = \frac{t_r V_{th}}{S}. \quad (2.2)$$

Setting the value of the threshold to $V_{th} = S_o/3$, where S_o is the most probable value of the signal amplitude, and assuming a signal variation of $S_o/3 < S < 5 * S_o$, then the delay can vary from $t_d = t_r$ for $S = S_o/3$ to $t_d = t_r/15$ for $S = 5S_o$.

We define the timing uncertainty due to time walk as the rms of the delay time distribution:

$$\sigma_t = [t_d]_{RMS} = \left[\frac{t_r V_{th}}{S} \right]_{RMS}. \quad (2.3)$$

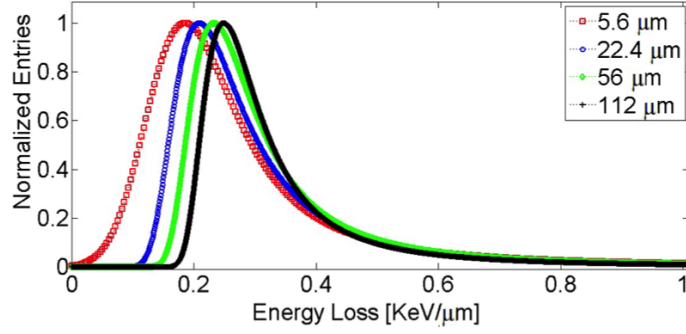


Figure 4. Average energy loss per micron of a ionizing particle in silicon layers of different thicknesses.

As it's clear from this expression, to minimize the effect of time walk we need to use the lowest possible value of the threshold. In the following we will use $V_{th} = 10 * N$, where N is the noise measured at the pre-amplifier output.

In silicon detectors, the amplitude S varies according to a Landau distribution. According to [8], the average energy loss per micron in the bulk of silicon decreases for thinner detector while the Landau width increases, Figure 4. The Landau Most Probable Value (mpv) and width ΔS for a detector of thickness d are given by:

$$mpv = 0.027 * \ln(d) + 0.126 \quad (2.4)$$

$$\Delta S/S = 0.7079 * d^{-0.266}. \quad (2.5)$$

Thin sensors suffer therefore of two additional problems with respect of thicker sensors: their average energy loss per micron is smaller and the variations are larger. Both these effects cause an enhanced time walk.

Using equations (2.4) and (2.5), it is possible to generate the appropriate Landau distribution for any given detector thickness. Figure 5 (top pane) shows the case of $d = 200\mu m$, while Figure 5 (bottom pane) shows the delay distributions for four different values of the threshold V_{th} , together with their RMS. The value of the time jitter for a shaping time of $t_r = 5500$ ps is therefore $\sigma_{TW} \sim 200 - 500$ ps, depending upon the chosen value of the threshold.

2.1.1 Time Walk Mitigation Techniques

The effect of time walk on the time determination can be greatly reduced if the signal amplitude is known. In this case, a correction function can be easily implemented. For this purpose, two techniques are commonly used: Time-over-Threshold (ToT) and Constant Fraction Discriminator (CDF). In this article we will not examine the details of these two techniques, however we will assume, very conservatively, that a factor of 3 in reduction of σ_{TW} can be achieved due to their use.

2.2 Jitter

Time uncertainty caused by the early or late firing of the comparator due to the presence of noise on the signal is called *jitter*. Figure 6 shows this effect.

Jitter is directly proportional to the noise N of the system and it is inversely proportional to the slope of the signal around the value of the comparator threshold. Assuming a constant slope we

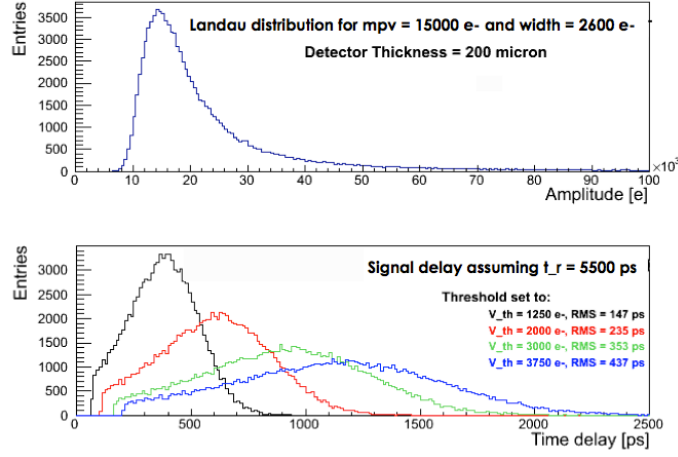


Figure 5. Top pane: Landau distribution of the energy lost by a minimum ionizing particle in a 200 μm thick silicon detector. Bottom pane: delay distributions for four different values of the threshold.

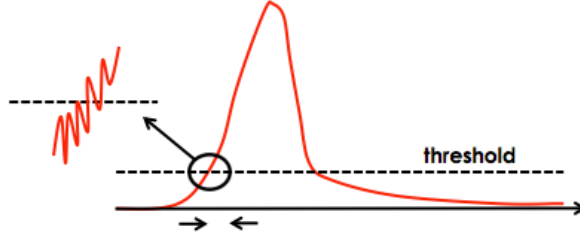


Figure 6. Noise causes an uncertainty on the time when the comparator fires.

can write $dV/dt = S/t_r$ and therefore:

$$\sigma_J = \frac{N}{dV/dt} = \frac{t_r}{S/N}. \quad (2.6)$$

3. A Parametrization of σ_t

Using the explicit expressions of σ_{TW} , σ_J and σ_{TDC} , equation 2.1 can be rewritten as:

$$\sigma_t^2 = \left(\left[\frac{t_r V_{th}}{S}\right]_{RMS}\right)^2 + \left(\frac{t_r}{S/N}\right)^2 + \left(\frac{TDC_{bin}}{\sqrt{12}}\right)^2. \quad (3.1)$$

Let's introduce the following quantities:

d: Detector thickness [micron]

l: Pixel pitch (assuming square pixels) [micron]

C_{Det} : Detector capacitance: $C_{Det} = \epsilon\epsilon_o \frac{l \cdot l}{d} + 0.2 \cdot 4l + 50$ fF.

The first term accounts for the capacitance to the back-plane, the second for the contribution from the neighbours and the third one for constant stray contributions.

Table 1. Dependence of various terms upon the preamplifier shaping time

Noise	$C_{Det}/\sqrt{t_r}$
Signal	$t_r < t_{col} \rightarrow S \propto t_r$ $t_r > t_{col} \rightarrow S \propto Const$
Threshold	$\propto N \propto C_{Det}/\sqrt{t_r}$.

N: Noise: $N \propto \frac{C_{Det}}{\sqrt{t_r}}$

We assume that is dominated by the voltage term.

S: Signal. The signal amplitude is determined by the detector thickness via equations 2.4 and 2.5.

t_r : Preamplifier rise time.

V_{th} : Comparator threshold. Set to 10 times the noise level: $V_{th} = 10 * N$

TDC_{bin} : TDC bin width. We consider a value of 20 ps.

3.1 Choice of Preamplifier Rise Time

Several effects such as the system noise N , the collected charge and the possibility to generate fake hits on neighbouring sensors should be considered when deciding the preamplifier rise time. In particular, the shaping time should be compared to the charge collection time (t_{col}) in the sensor to evaluate the amount of charges collected within t_r : the signal S increases until $t_r \sim t_{col}$ while it's a constant for $t_r > t_{col}$. Table 1 shows explicitly the dependence of several factors of equation 3.1 upon t_r .

Using the expressions of Table 1 in equation 3.1, we can derive the dependence of σ_t upon t_r :

$$t_r < t_{col} \rightarrow \sigma_t \propto \frac{C_{det}}{\sqrt{t_r}} \quad (3.2)$$

$$t_r > t_{col} \rightarrow \sigma_t \propto C_{det} * \sqrt{t_r}. \quad (3.3)$$

Assuming a detector thickness of 100 micron, with a collection time $t_{col} = 1250$ ps, Figure 7 shows the time resolution σ_t for an $l = 100 \mu\text{m}$ pixel as a function of the amplifier shaping time t_r .

Time resolution is therefore minimized for $t_r \sim t_{col}$, relation that will be always used in the remaining part of this paper.

4. Results

The interplay among key parameters of equation 3.1 is shown in Figure 8. The detector thickness d and pixel size l determine the capacitance C_{det} and shaping time t_r , which in turn determines, together with C_{det} the noise N . The curves have been normalized to the existing NA62 Gigatracker system [10]: $d = 200 \mu\text{m}$; $l = 300 \mu\text{m}$; $t_r = 5500$ ps and $N = 300 e^-$, accounting for the fact that the Gigatracker shaping time it's longer than the collection time.

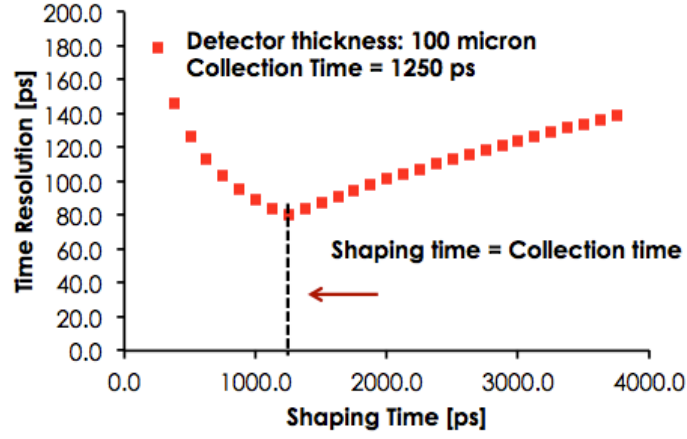


Figure 7. Time resolution σ_t for an $l = 100 \mu\text{m}$ pixel as a function of the amplifier shaping time t_r .

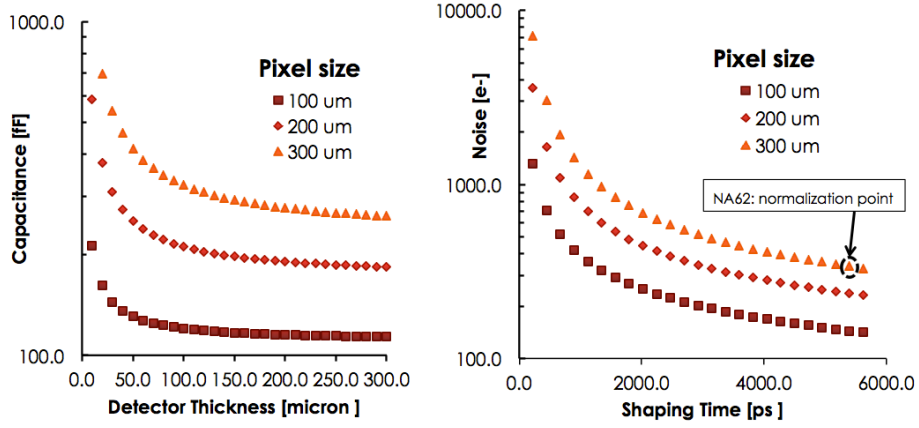


Figure 8. Interplay among key parameters of the parametrization of σ_t .

4.1 State of the Art

With the assumptions outlined above, the state of the art of timing capability in silicon sensors is shown in Figure 9. The left (right) pane shows σ_t , and its two parts σ_{TW} and σ_J , for a $l = 300 \mu\text{m}$ ($l = 100 \mu\text{m}$) pixel sensor as a function of detector thickness. The contribution from time walk has been reduced by a factor of three, considering the effect of a ToT or CFD circuit. The secondary x-axis at the top of each plot shows the appropriate shaping time.

Our parametrization shows that the best time resolution is obtained for thicker sensors, driven by higher signals, while larger pixel size have worse time resolution due to their higher capacitance. We find $\sigma_t \sim 100 \text{ ps}$ for a $l = 300 \mu\text{m}$ pixel sensor of 250-300 μm thickness, while, for the same sensor thickness but a pixel size of $l = 100 \mu\text{m}$ we obtain $\sigma_t \sim 50 \text{ ps}$.

4.2 Ultra-Fast Silicon Detector

As equation 3.1 shows, the key to better time resolution is the possibility to increase the S/N ratio. Exploiting the larger signal from LGAD, we foresee the possibility to build ultra-fast silicon detectors. In the following we will assume that the S/N ratio in UFSD increases by a factor of 10,

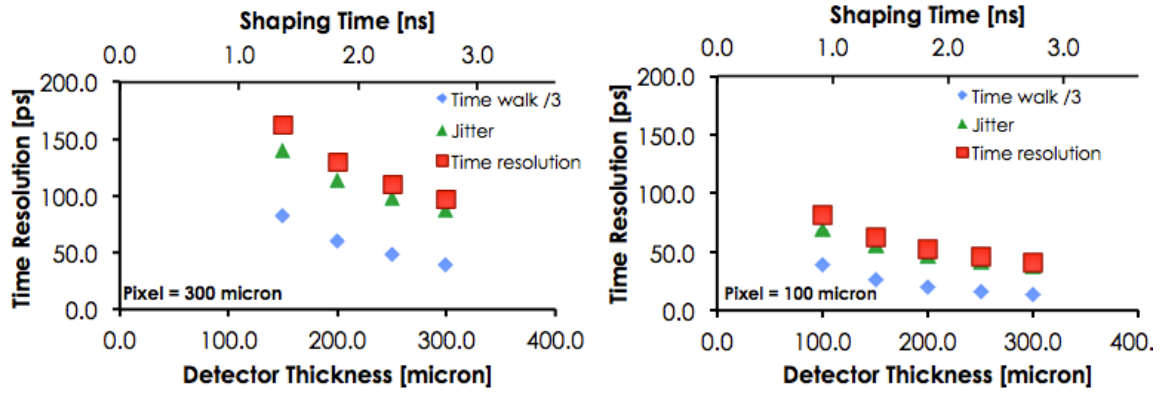


Figure 9. The left (right) pane shows σ_t , and its two parts σ_{TW} and σ_J , for a 300 μm (100 μm) pixel sensor as a function of detector thickness.

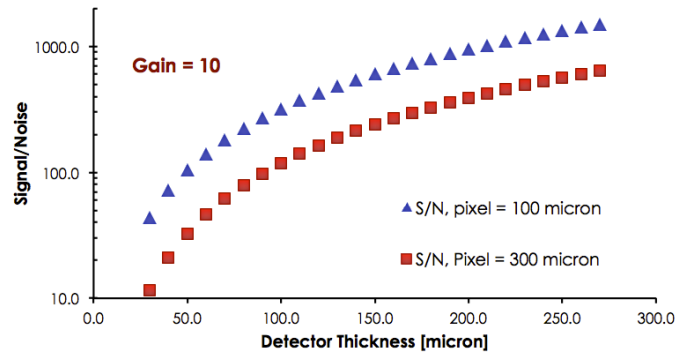


Figure 10. S/N ratio for a $l = 100 \mu\text{m}$ and a $l = 300 \mu\text{m}$ pixel detector as a function of the detector thickness for an UFSD with gain = 10.

obtained by means of a larger signal without an equivalent increase of the noise. Figure 10 shows the S/N ratio for a $l = 100 \mu\text{m}$ and a $l = 300 \mu\text{m}$ pixel detector as a function of the sensor thickness for an UFSD with gain = 10.

It's important to notice that charge collection time t_{col} for UFSD is actually longer than that in traditional pixel detectors, as it comprises of the usual time drift of the charges towards the respectively electrodes, plus the time taken by the holes produced in the the multiplication layer to drift back to the p^{++} electrode.

The effect of the increased S/N ratio in UFSD is visible in Figure 11(left pane), where a time resolution $\sigma_t < 20 \text{ ps}$ is achieved for detector thicknesses above $d = 50 \mu\text{m}$ for a $l = 100 \mu\text{m}$ pixel, while a $l = 300 \mu\text{m}$ pixel detector reaches an analogous time resolution for thicknesses above $d = 150 \mu\text{m}$.

A very large S/N is also a great benefit for time-walk correction: as the signal S increases while the threshold V_{th} does not change, the time-walk becomes quite small. The time resolution σ_t without any time-walk mitigation circuit is shown in Figure 11 (right pane) for a $l = 100 \mu\text{m}$ pixel size: a time resolution of less that 20 ps is achievable for detector thicknesses above 100 μm . The possibility to have good time resolution without time walk correction greatly simplifies the associated electronics, allowing for smaller pixels and lower power consumption.

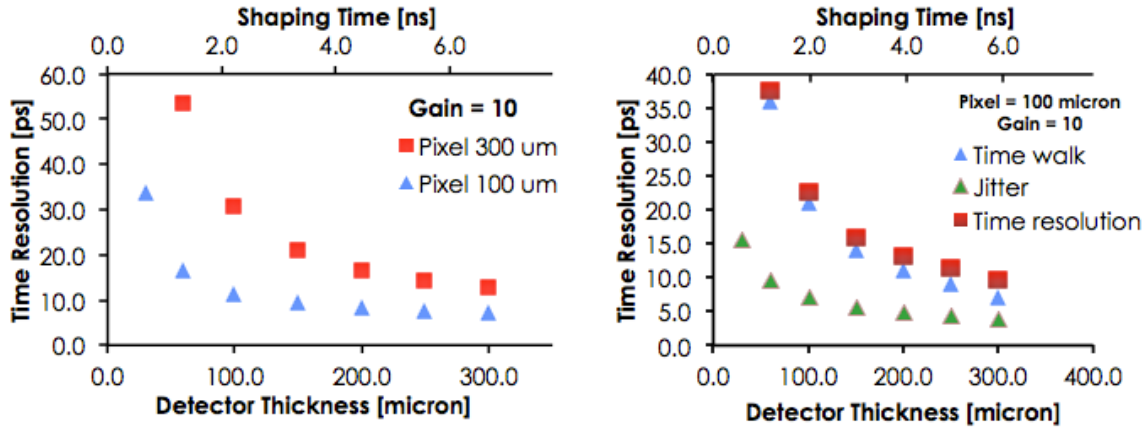


Figure 11. Time resolution σ_t for two different pixel sizes ($l = 100 \mu\text{m}$ and $l = 300 \mu\text{m}$) as a function of the detector thickness for a UFSD with Gain = 10. Right pane: time resolution σ_t for a pixel sizes of $l = 100 \mu\text{m}$ without any time walk mitigation circuit, as a function of the detector thickness for a UFSD with Gain = 10.

4.2.1 Additional Sources of Timing Errors

Time Walk addresses the impact of amplitude variations on σ_t while the jitter term parametrizes the effect of system noise. There are also additional effects that might contribute to σ_t by modifying the shape of the signal, for example track location and direction, variation of ionization location along the track, δ rays and diffusion [9]. These effects are, however, minimized by the geometry of planar pixel sensors as the Ramo weighing field is, contrary to 3D detectors, almost constant within the bulk and the drift velocity is always saturated.

5. Summary

We propose a parametrization to evaluate the timing performance of Ultra-Fast Silicon Detectors, based on the LGAD concept. The increased S/N ratio is the key for the excellent timing performance. Figure 12 presents our findings: thicker detectors have better time resolution, at a price of higher occupancy, as the drift time is longer. Smaller size pixels, due to the lower capacitance value, offer better performances. The combination of small size pixels ($l < 150 \mu\text{m}$) and thick detector ($d \sim 200 - 300 \mu\text{m}$) allows for a simplified electronics, as the time-walk compensating circuit might not be necessary.

Acknowledgments

The authors wish to thank Gian-Franco Dalla Betta and Gregor Kramberg for their insights and suggestions.

References

- [1] RD50 collaboration, <http://rd50.web.cern.ch/rd50/>.

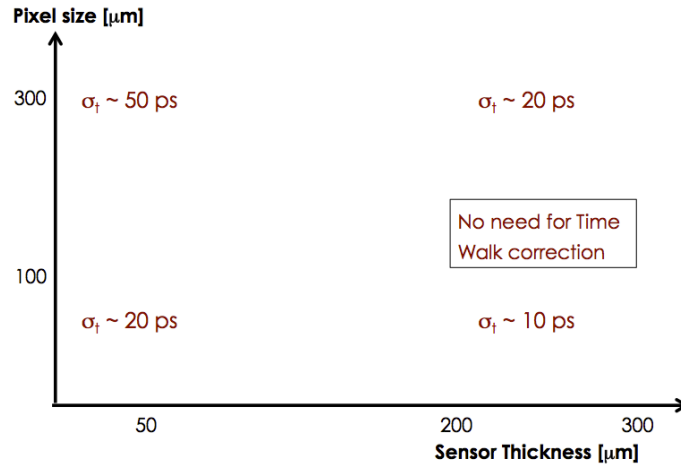


Figure 12. Summary of the results obtained with our parametrization: thicker detectors have better time resolution, at a price of higher occupancy, as the drift time is longer. Smaller size pixels, due to the lower capacitance value, offer better performances. The combination of small size pixels ($l < 150 \mu\text{m}$) and thick detector ($d \sim 200 - 300 \mu\text{m}$) allows for a simplified electronics, as the time-walk compensating circuit might not be necessary.

- [2] P. Fernandez, et al, *Simulation of new p-type strip detectors with trench to enhance the charge multiplication effect in the n-type electrodes*, Nucl. Instrum. Meth. A658 98-102 (2011).
- [3] G. Pellegrini et al., *Technology developments and first measurements of Low Gain Avalanche Detectors (LGAD) for High Energy Physics applications*, Hiroshima Conference, HSTD9, Hiroshima, Japan. Nucl.Instrum.Meth A, in print.
- [4] H. F.-W. Sadrozinski, *Exploring charge multiplication for fast timing with silicon sensors*, 20th RD50 Workshop, Bari, Italy, May 30-June 1, 2012, and references therein <https://indico.cern.ch/conferenceOtherViews.py?view=standard&confId=175330>.
- [5] H. F.-W. Sadrozinski, et al., *Ultra-Fast Silicon Detectors*, RESMDD12, Nucl.Instrum.Meth A, in print.
- [6] H. F.-W. Sadrozinski, et al., *Sensors for Ultra-Fast Silicon Detectors*, HSTD9, Hiroshima, Japan. Nucl.Instrum.Meth A, in print.
- [7] A. Rivetti, et al., *Electronics for Fast Tracking Detector*, HSTD9, Hiroshima, Japan. Nucl.Instrum.Meth A, in print.
- [8] S. Meroli et al, *Energy loss measurement for charged particles in very thin silicon layers 2011 JINST 6* P06013
- [9] S. Parker et al., *Increased speed: 3D silicon sensors; fast current amplifiers*, IEEE Transaction on Nuclear Science, Vol. 58, No 2 April 2011.
- [10] E Martin et al, *Review of results for the NA62 gigatracker read-out prototype 2012 JINST 7* C03030